Correlated Excimer Formation and Molecular Rotational Dynamics in Phenylacetylene Dendrimers†

Stephen F. Swallen,‡,|| Zhengguo Zhu,§ Jeffrey S. Moore,§ and Raoul Kopelman*,‡

Department of Chemistry, University of Michigan, Ann Arbor, Michigan 48105 and Department of Chemistry, University of Illinois, Urbana, Illinois 61801

Received: December 6, 1999

Steady-state and time-resolved fluorescence data are used to examine the photophysical characteristics of a series of phenylacetylene dendrimers. Correlated excimer formation is observed in some solvents which is found to depend strongly upon initial excited-state placement within the dendrimer framework. The results suggest two distinct solvated molecular environments which give rise to independent photophysical behaviors. Models of excimer formation dynamics and relaxation kinetics are described. Additionally, fluorescence anisotropy measurements are examined in the context of simultaneous probe wobbling-in-a-cone and macromolecular dendrimeric rotation as the mechanisms leading to fluorescence depolarization. Approximate solutions to the model are shown to provide good descriptions of the solvated molecular dynamics.

I. Introduction

The synthesis, study, and practical usage of increasingly sophisticated supermolecular dendrimer systems has progressed rapidly in recent years. A wide variety of important applications are being addressed with these new molecules, including potential drug delivery systems,[1,2] electrooptical organic light sources,[3] and even nanometer scale optical chemical sensors.[4−6] Recently we have investigated a class of purely hydrocarbon dendrimers composed of repeat phenylacetylene (PA) units. Two series of dendrimers have been examined: the "compact" series with ideal fractal (dilation) symmetry, in which all dendrimeric subunits are composed of identical single PA chains, and the "extended" series which have PA linear chains that increase in length toward the molecular locus. In both cases, due to the meta-position branching geometry at each node, these dendrimers exhibit excited-state localization along individual PA chain units.[7,8] Thus, it is possible to observe exciton hopping between states. In addition, we have shown previously[9] that due to the subtle change in molecular geometry between the compacts and extendeds, these two groups display markedly different energetic behavior. In particular, the extended dendrimers show greatly enhanced energy funneling capabilities due to molecular geometry, with nearly unit quantum yield of exciton transfer from the dendrimer backbone to a perylenic trap substituted at the molecular core.[9] In contrast, the compacts exhibit a bias for exciton hopping out toward the dendrimer periphery (rather than toward the locus), resulting in greatly decreased rates and efficiencies of exciton trapping.

The phenylacetylene dendrimers and their perylenic-substituted derivatives have been closely studied both theoretically[10,11] and experimentally[8,9,12] with respect to the energetic absorption and funneling characteristics. The extended molecules, with the inherent thermodynamic bias for exciton trapping at the molecular locus, exhibit much more rapid and efficient directional funneling of absorbed radiation in comparison to the compact series. This funneling behavior has been observed to vastly increase the trapping photoefficiency in several supermolecular systems[13−15] and may provide a useful means for interconversion of electrical, optical, and chemical energy. In addition to these favorable characteristics, some quite unexpected photophysical phenomena have also been observed. This paper discusses these unusual light-induced characteristics and the molecular reorientational dynamics of these dendrimer supermolecules that have recently been studied in solution. The first section deals with the study of excited-state dimers that are seen even at extremely low concentrations in certain solvents. Quite unexpectedly, however, these systems exhibit an excimer/monomer fluorescence intensity ratio that is acutely dependent upon excitation wavelength. The relative degree of excimer formation is dependent not only upon overall dendrimer concentration but also upon which one of the localized dendrimer states is initially excited. The solvated molecular dynamics of excimer formation are discussed, and a model of the independent excited-state relaxation pathways for the monomer and excimer species is presented. The second discussion section of this paper presents fluorescence anisotropy results that provide intramolecular librational motion correlation times of the fluorescent trap and rotational times for macromolecular reorientation in solution. The data are analyzed on the basis of a model of a restricted rotor which "wobbles" about its principal axis, coupled to a more slowly rotating macromolecule.[16,17]

II. Experimental Section

The synthesis of the compact and extended phenylacetylene dendrimers has been presented in detail previously.[18] Figure 1 shows the ethynylperylene-substituted compacts W15-per, W31-per, and W63-per, composed of 3, 4, and 5 generations, respectively, and a corresponding extended dendrimer dubbed the nanostar. Samples were prepared in spectrophotometric grade dichloromethane and *n*-hexane (Aldrich and Fisher) by serial

† Part of the special issue "Harvey Scher Festschrift".
* Corresponding author.
‡ University of Michigan.
§ University of Illinois.
|| Present address: Department of Chemistry, University of Wisconsin, Madison Wisconsin 53705

10.1021/jp994284p CCC: $19.00
Published on Web 04/04/2000

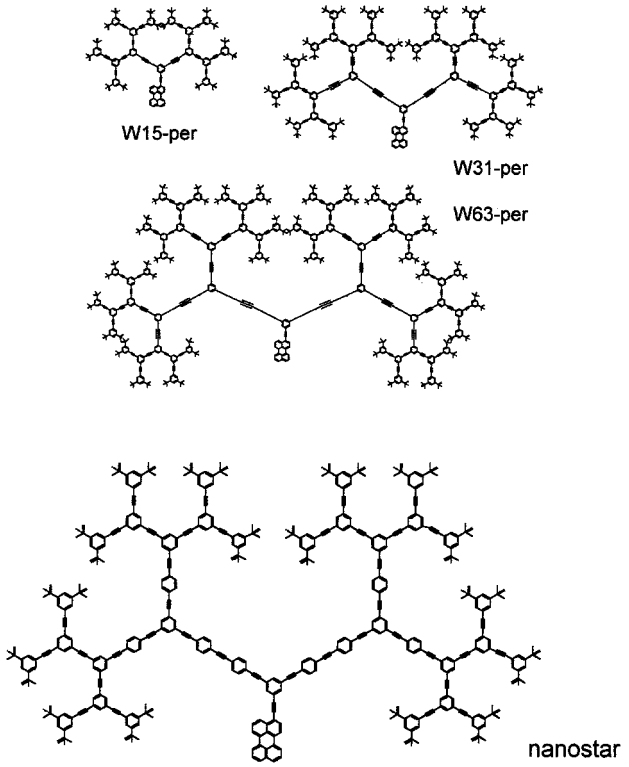

Figure 1. (A, top) Series of three compact perylene-substituted derivatives. Dendrimers of 3-, 4-, and 5-generations are shown. These are named according to the number of phenyl rings in the dendrimer backbone, W15-per, W31-per, and W63-per, respectively. Other members of this series have also been synthesized, including W7-per and W127-per. (B, bottom) An extended perylene-substituted dendrimer referred to as the "nanostar", which has increasing length linear phenylacetylene chains toward the locus.

dilution from stock solutions. Excited-state quenching by oxygen was avoided by bubbling solutions with N_2. Steady-state fluorescence measurements were conducted on an ISS Fluorolog2. The fluorescence anisotropy was obtained by a standard time-correlated single photon counting procedure in reverse-time mode. An argon ion pumped titanium−sapphire laser (Spectra-Physics Tsunami) was externally electrooptically pulse picked (Conoptics) at 2 MHz and then frequency doubled and tripled (GWU). A microchannel plate photomultiplier tube (Hamamatsu 3809-50) was used for signal detection. Pulse discrimination (EG&G Ortec 9307) and time analysis (EG&G Ortec 9308) provided instrument response curves of typically 60 ps full width at half-maximum, which were used for the deconvolution of excited-state fluorescence lifetime measurements. Best fits to the data were found using a Marquard least-squares fitting routine.[19]

The laser excitation pulse was linearly polarized, with a wavelength around 435 nm (typically 150 fs), to directly excite the vibrationless singlet electronic transition of the phenylethynylperylene (PEP) trap. Excitation wavelengths of 390, 334, and 300 nm were also used for excitation of the individual dendrimer states for both the excimer studies and to examine the fluorescence depolarization dynamics. Fluorescence lifetime data for both the dendrimeric monomer (measurements made at the vibronic peaks at 480 and 515 nm) and excimer (580 nm) were made with the detection polarizer set at the magic angle (54.7°). Fluorescence anisotropy data were taken with the detection polarizer alternately aligned parallel and perpendicular to the excitation polarization.

The polarization bias of the system, known as the G factor, was found using the tail-matching procedure[20] on perylene and other reference dyes in several solvents. It was reproducibly found to be $G = 1.02$. This value was used for intensity correction of the perpendicularly polarized detection data, $I_\perp(t)_{\text{corrected}} = GI_\perp(t)_{\text{measured}}$. The corrected curves were used in all calculations discussed below.

III. Results and Discussion

A. Excited-State Dynamics and Excimer Formation. Recent experimental data[21] have provided evidence of a highly unusual mechanism of excimer formation. In addition to expected solvent and concentration dependencies, the excimer concentration is found to be extremely dependent upon excitation wavelength. These data will be discussed here with a more detailed kinetic discussion of exciton dynamics given below.

Steady-state monomer and excimer fluorescence intensities were measured across 4 decades of concentration in *n*-hexane. While no ground-state dimer formation was observed with absorption spectroscopy below 10^{-5} M, significant excimer formation was seen even at very dilute concentrations[22] ($<10^{-9}$ M). It should be noted that a significant solvent effect was observed: while *n*-hexane solutions demonstrated enhanced excimer formation, only a very low excimer concentration was observed in cyclohexane, and no excimer formation was seen at any dendrimer concentration in dichloromethane.

Fluorescence spectra were measured following excitation into one of the four electronic excited states of the nanostar molecule. Previous experiments[7,9] and theoretical calculations[11] have shown that due to the meta-position branching pattern at each dendrimer node, there is a nearly complete loss of conjugative delocalization between neighboring phenylacetylene (PA) chains. An effective barrier is introduced between the π-electron excitations of neighboring PA units, breaking the resonative conjugation among the benzene rings. Thus, photoinduced excitons are initially localized on a single chromophoric unit, composed of an individual linear PA chain. In addition, the varying lengths of the dendrimer states create a thermodynamic gradient, resulting in an excitonic funnel toward the PEP moiety. Thus, all localized excitons rapidly transfer to the molecular locus, giving rise to fluorescence only from the trap at the center.

Figure 2 shows the fluorescence spectra of 7.0×10^{-8} M solutions following excitation into each of the nanostar states. The PEP trap absorption is centered at 450 nm, while the localized dendrimer states are at 390, 334, and 300 nm for decreasing length linear PA chains of 4, 3, and 2 units, respectively.[7] (As can be seen in Figure 1, the longest PA chains are adjacent to the central PEP trap, while the shortest, highest energy chains are located at the periphery.) The excitation wavelengths were chosen such that each electronic state was excited uniquely during each measurement. The spectra have been normalized to the vibrationless radiative relaxation peak intensity at 480 nm. This permits a direct intensity comparison, which takes into account the wavelength dependence of extinction coefficients due to the number of absorbing units (which go as 2^n, where n is the dendrimer generation number), and the fluorescence quantum efficiency, which is governed by the trapping efficiency from each dendrimer state. The data show the three expected perylenic vibronic peaks[23] due to nanostar monomer relaxation, as well as a broad structureless peak centered at 580 nm. This latter red-shifted feature is due to radiative decay of an excited-state pair, formed by the overlap

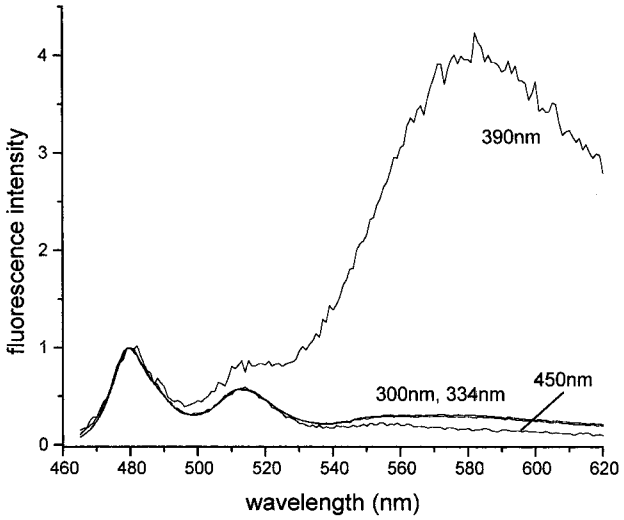

Figure 2. Steady-state fluorescence spectra of nanostar following excitation at four wavelengths, at 7.0×10^{-8} M in deoxygenated *n*-hexane. The curves have been normalized to the peak intensity of the vibrationless $S_1 \rightarrow S_0$ fluorescence transition at 480 nm. The wavelengths correspond to unique excitation of the four localized states of the extended dendrimer: perylenic trap at 450 nm, innermost, middle, and peripheral dendrimer generations at 390, 334, and 300 nm, respectively. Fluorescence peaks due solely to monomeric nanostar species are observable at 480, 515, and 552 nm. Excimer fluorescence is the broad structureless peak centered around 580 nm. The ratio of excimer-to-monomer fluorescence intensity is unexpectedly large for excitation at 390 nm.

TABLE 1: Ratio of Excimer-to-Monomer Peak Intensities, Following Excitation of Each Dendrimer Generation in *n*-Hexane at 7×10^{-8} M

excitation wavelength, nm	dendrimer generation	excimer/monomer ratio
310	3	0.33
334	2	0.31
390	1	4.0
450	trap	0.14

of two neighboring nanostar molecules *at the perylenic locus*, and has the typical perylenic excimer features.[24]

Of particular note is the strong dependence of excimer fluorescence intensity on initial excited state. The perylenic excimer intensity is more than an order of magnitude greater when the molecule is excited into the innermost dendrimer state than when excited directly into the PEP moiety (see Table 1.) This suggests that an energetically preferred nearest-neighbor approach of electronic ground-state nanostars in solution causes a simultaneous proximity between the lowest energy dendrimer generations (longest chains), as illustrated in Figure 3. Excitation into this state preferentially enhances the creation of perylenic state excimer formation. This dynamic pathway allows the minimization of the energy barrier to excimer formation: the center of mass of each of the dendrimers remains fairly stationary, while augmented librational motion of the trap moieties creates the excited-state dimer in a geometrical configuration that is favorable to excimer formation.

It is also notable that the excimer intensity decreases when initially exciting into the outer dendrimer states. On the basis of the energy funneling mechanism previously discussed,[9,21] it would be expected that excitations into any dendrimer state would pass through the lowest energy PA chain before being trapped at the locus. The results of Figure 2 indicate that a direct transfer of excitons from the periphery states to the trap may occur to some degree, bypassing the interior of the dendrimer

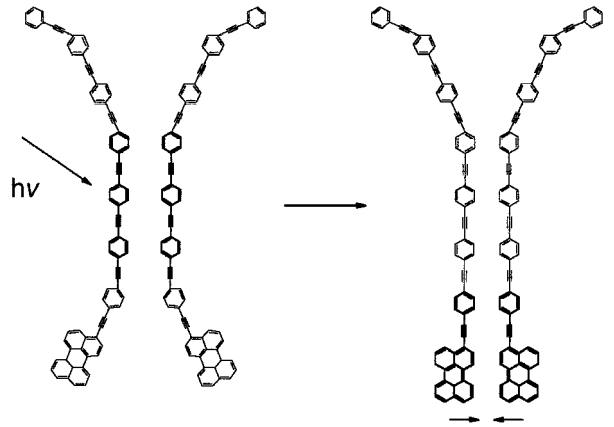

Figure 3. Schematic view of excimer formation dynamics of the nanostar in *n*-hexane. Photoexcitation of the innermost dendrimer state (left) enhances molecular electronic excited-state pair formation, creating an excimer involving the perylenic trap states (right).

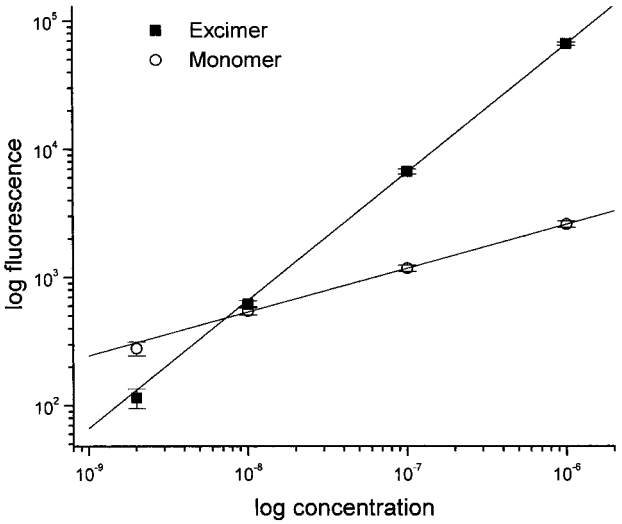

Figure 4. Concentration dependence of the steady-state fluorescence intensity of nanostar in *n*-hexane. The open circles are the monomer detected at 480 nm, and the solid squares are the excimer detected at 580 nm, both following excitation directly into the lowest energy dendrimer state at 390 nm. The solid lines are the least-squares best fit and have slopes of 0.22 for the monomer and 1.0 for the excimer.

backbone. This "excitation short circuit" has been discussed in the context of the molecular structural folding of the dendrimer, which results in a globular solvated shape.[25] This formation allows close spatial contact between the periphery states and the molecular trap, permitting a short-range Forster-like through-space exciton transfer pathway. As the exciton mostly avoids passing through the lowest energy dendrimer state, the enhancement of excimer formation is highly reduced. As Table 1 shows, the excimer/monomer fluorescence intensity ratio following excitation at the nanostar periphery is only a factor of 2 or 3 higher than following direct excitation of the PEP trap.

The peak monomer and excimer fluorescence intensities were further examined as a function of total dendrimer concentration. Models of two-body interaction kinetics typically used to describe excimer formation predict a squared dependence of excimer fluorescence intensity on concentration, while the monomer increases linearly. However, a more complicated scenario has been observed. Figure 4 gives a double-log plot of fluorescence peak intensity versus total dendrimer concentration following excitation into the lowest energy dendrimer state. Unexpectedly, the excited-state pair fluorescence was measured

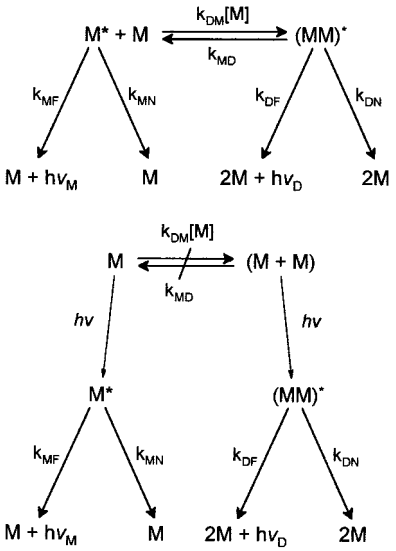

Figure 5. (A, top) Kinetic scheme describing excimer formation in solution (after Birks[23]). On the basis of this model, both the monomer and excimer fluorescence lifetime data are expected to be biexponential, given by eq 1. (B, bottom) Proposed kinetic scheme for the photoexcitation and relaxation pathways of monomeric, M*, and excimeric, (MM)*, nanostar in *n*-hexane. The species (M + M) and (M* + M) indicate a close spatial arrangement of electronically noninteracting ground-state and excited-state molecules, respectively.

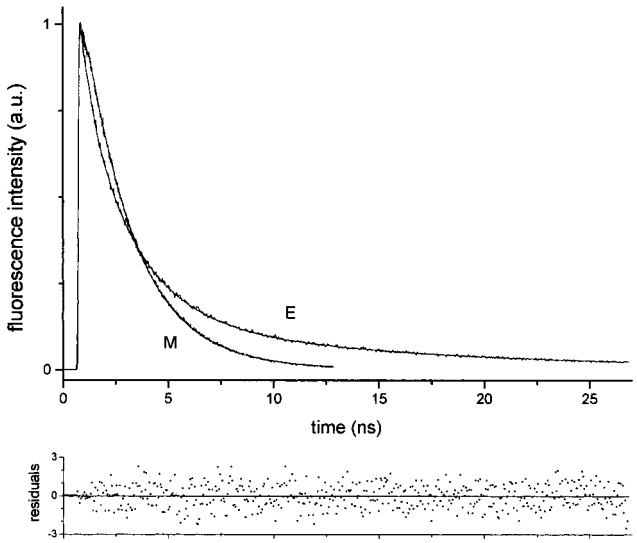

Figure 6. Fluorescence lifetime decay of 1.0×10^{-7} M nanostar in deoxygenated *n*-hexane, following excitation at 430 nm. The curves are for the monomer (M) species detected at 480 nm and the excimer pair (E) at 580 nm. The best fit curves to the data are given as solid lines. The monomer was fit to a single exponential of 2.4 ns, while the excimer was fit to a biexponential $A_1 = 0.85$, $\tau_1 = 2.1$ ns, $A_2 = 0.15$, $\tau_2 = 12$ ns.

to increase linearly (slope = 1.0), while the monomer was quite sublinear (slope = 0.22). This is particularly surprising given that previous absorption spectra provide no indication of ground-state dimer formation and that the absorption intensity of the monomer increases nearly linearly over this concentration range (slope = 0.9). The traditional model elucidated by Birks[23] assumes an equilibrium reaction between the monomer and excimer that is fast on the time scale of the excited state. The data indicate that on this time scale we do not have this equilibrium, and the observed dendrimeric excimers are not formed by collision-induced dimerization between an excited-state and a ground-state molecule. In conjunction with the time-dependent data discussed immediately below, these data suggest a lack of equilibrium between isolated ground-state monomers and a weakly associated noninteracting ground-state pair, at least within the time frame of the electronic excitation dynamics.

This complex excited-state behavior of the nanostar in *n*-hexane was examined further using time-dependent fluorescence lifetime measurements. For freely diffusing particles in solution, it is fairly straightforward to express the kinetic scheme and solve for the time-dependent fluorescence intensity at the monomer (480 nm) and excimer (580 nm) wavelengths.[23] This is demonstrated in Figure 5A, where k_{MF} and k_{MN} are the radiative and nonradiative decay constants for the monomer, k_{DF} and k_{DN} are the same for the excimer, and k_{DM} and k_{MD} are the rate constants for exchange between monomer and excimer states. Following a δ-function excitation pulse, the initial monomer and excimer concentrations are $[M^*] = [M^*]_0$ and $[D^*] = 0$, and time-dependent kinetic rate equations can be expressed on the basis of the decay processes shown in Figure 5A. Solutions to the rate equations for these quantities provide the molecular fluorescence response functions

$$i_M(t) = A_1 \exp(-\lambda_1 t) + A_2 \exp(-\lambda_2 t) \quad (1a)$$

$$i_D(t) = A_D[\exp(-\lambda_1 t) - \exp(-\lambda_2 t)] \quad (1b)$$

where A_1, A_2, and A_D are the relevant amplitude terms. The exponential terms λ_1 and λ_2 are given as

$$\lambda_{1,2} = {}^1/_2(k_{MF} + k_{MN} + k_{DM}[M] + k_{DF} + k_{DN} + k_{MD}) \mp {}^1/_2\{(k_{DF} + k_{DN} + k_{MD} - k_{MF} - k_{MN} - k_{DM}[M])^2 + 4k_{MD}k_{DM}[M]\}^{1/2} \quad (2)$$

Thus, for simple molecular systems with no ground-state dimer formation (only a statistical collision probability of monomers) and an equilibrium between excited-state species (monomer and excimer), the monomer fluorescence decay is the sum of two exponential terms, while the excimer decay is the difference between the same two terms. Following deconvolution of the data with the measured instrument response function, the two decay parameters λ_1 and λ_2 may be determined from the fluorescence decay functions of both species. However, the experimental data for the nanostar molecule in *n*-hexane are not fit by this model and instead suggest a more involved kinetic scheme. Figure 6 gives the measured decays for both monomer and excimer species, along with the calculated best fit. While the excimer fluorescence decay is well fit by a biexponential function ($A_1 = 0.85$, $\tau_1 = 2.1$ ns; $A_2 = 0.15$, $\tau_2 = 12$ ns), the monomer decay was optimally fit by a single exponential ($\tau = 2.4$ ns). Within the fitting resolution, the measured lifetimes of both species are independent of dendrimer concentration up to concentrations $\geq 10^{-7}$ M. Thus, the rate constants for monomer/excimer equilibration (k_{DM} and k_{MD}) must be vanishingly small. This suggests that two independent populations[26] relating to two distinct solvation environments are present in solution, leading to the photoexcitation of the two species, as shown in Figure 5B. While they both initially have the same absorption and fluorescence spectral features and distributions, the resulting kinetics pathways are different. One type consists of fully solvated, completely isolated nanostar molecules (M*) which simply decay back to the electronic ground state via fluorescence. The second type of photoexcited molecules is in close spatial proximity to another nanostar. This weakly associated excited-state pair (M* + M) gives rise to the observed excimer

(MM)*. While in the ground state, the members of this geminate pair are sufficiently independent that there is no evidence of dimer formation in absorption spectra,[7] but electronic overlap induced by photoexcitation gives rise to the longer wavelength excimer fluorescence. The rate of excited-state dimer formation is quite rapid (fast on the nanosecond time scale of the lifetime measurements), and the resulting product is sufficiently energetically downhill from the weakly bonded "pair" that monomer fluorescence from this subset of molecules is effectively quenched.

An additional comparison of the results with the Birks model may help to emphasize and partially elucidate the unusual photoinduced dynamics of this molecular system. In the (unlikely) case that the decay parameters are nearly degenerate ($\lambda_1 \approx \lambda_2$), the monomer fluorescence response function $i_M(t)$ would be observed as a single exponential. This explanation, however, does not concur with the observed concentration dependence of the fluorescence decay measurements. No changes in the lifetimes were observed experimentally over more than 2 decades of concentration (10^{-9} to 5×10^{-7} M). This contrasts with the low concentration limit of eq 2, where as ground-state dendrimer concentration [M] $\rightarrow$ 0, the decay parameters simplify to

$$\lambda_1 \rightarrow k_{MF} + k_{MN} \tag{3a}$$

$$\lambda_2 \rightarrow K_{DF} + k_{DN} + k_{MD} \tag{3b}$$

λ_1 is then dependent only upon the natural decay rates of the isolated monomer, while λ_2 depends only upon the excimer excited state. In this event, degeneracy is certainly not to be expected.

We suggest the kinetic scheme in Figure 5B as a reasonable alternate proposal, based on a negligible rate of interchange between the monomer and excimer states. Following photoexciation, the isolated monomers decay back to the ground state, giving rise to a single-exponential decay function. The biexponential nature of the excimer data may still be expected due to a multistage mechanism of pair formation (such as a structural rearrangement and alignment of submolecular units, sequentially followed by electronic state overlap).

A fundamental question relating to the origin of this effect is then raised, specifically relating to why the monomer and excimer state appear to have independent kinetic pathways and the lack of equilibration between the two environments. Although the answers to this are still quite cloudy, it is worth reiterating the solvent-dependent nature of these results. The most significant excimer formation was seen in *n*-hexane, much less in cyclohexane, and not at all in dichloromethane. A consistent pattern was also seen with regard to the overall solubility of the dendrimers (least in *n*-hexane) and also to a lesser degree with fluorescence quantum yield (greatest in dichloromethane).

The combination of steady-state and time-resolved spectral data for the nanostar dendrimer in *n*-hexane strongly suggests that, in this solvent, we have a preponderance of geminate molecular pairs. Following photoexcitation, the electronic intermolecular overlap leads to excimer formation. Of particular interest is the strong wavelength dependence of this pairing: while the excimer fluorescence is observed solely from the perylenic trap, the excited-state pair is most efficiently formed by initial excitation into the lowest energy dendrimer state. This unusual excimer species has provided information regarding the energy trapping mechanism in these thermodynamic funnel molecules, as well as the solvation characteristics in several solvents.

B. Fluorescence Anisotropy and Molecular Reorientation. Time-dependent fluorescence anisotropy was utilized to provide information on molecular motion and structure in solution. The nanostar and the series of compact perylenes pictured in Figure 1 were examined at low concentration in dichloromethane solutions and showed no evidence of intermolecular interactions, such as dimer or excimer formation or long-range energy transfer. By exciting directly into the phenylethynylperylene (PEP) trap, the observed fluorescence depolarization is due to rotational reorientation of the entire dendrimer molecule and simultaneous intramolecular motions of the PEP moiety. These factors will be discussed in more detail below. In the hydrodynamic limit, the macromolecular rotation time, τ_r, can be approximated using the Debye−Stokes−Einstein equation, given as

$$\tau_r = 1/6D_r = V\eta/kT \tag{4}$$

Here D_r is the rotational diffusion constant, V is the molecule assumed to be a sphere, and η is the solvent viscosity. While the dendrimers are graphically depicted as planar, they are typically globular shaped in solution, with radii of roughly 2−4 nm. These calculations can be compared to values obtained for the macromolecular rotation times via fluorescence anisotropy measurements below.

The measurement of parallel ($I_{||}(t)$) and perpendicular ($I_{\perp}(t)$) fluorescence data for the dendrimer molecules permits the calculation of the time-dependent anisotropy

$$r(t) = [I_{||}(t) - I_{\perp}(t)]/[I_{||}(t) + 2I_{\perp}(t)] \tag{5}$$

This is done by first fitting the parallel and perpendicular curves independently to arbitrary fitting functions, allowing the calculation of $r(t)$ using deconvolved curves. This permits the fitting of the anisotropy free from instrument response effects and the excited-state fluorescence decay lifetime. The reliability of the data and the polarization sensitivity of the detection system can be checked by comparing the denominator in eq 5 to the excited-state lifetime of the fluorescent probe measured at the magic angle. The normalized total fluorescence $F(t) = [I_{||}(t) + 2I_{\perp}(t)]$ should reproduce the single-exponential decay observed for the fluorescence lifetime. This was done for isolated perylene and for all the dendrimer samples, with identical curves for the two measurements within the data resolution.

If at some time after excitation the fluorophore's emission dipole, μ_e, has an angle ϕ with respect to the absorption dipole μ_a at time $t = 0$, the instantaneous anisotropy is

$$r = {}^1/_5(3\cos^2\phi - 1) \tag{6}$$

and thus the maximum value for collinear dipoles at the moment of excitation is $r_0 = {}^2/_5$. Previous measurements of isolated perylene in various solvents[27,28] have found values for $r_0 = 0.30-0.34$. As a test, our measurements of perylene in dichloromethane found values of $r_1 = 0.11$, $r_2 = 0.21$, and $r_0 = r_1 + r_2 = 0.32$. (While the measured rotational times that correspond to these factors are solvent-dependent, the magnitudes of the r values are not, and these are found to agree well with previous works. See Christensen et al.[28] for a fuller discussion.) As shown in Figure 7, this suggests an angle ϕ_{ae} between the absorption dipole (oriented along the long molecular axis) and the emission dipole at $t = 0$ of about 22°. As expected due to the localized electronic structure of the dendrimers, very similar values were measured for isolated ethynylperylene and for the directly excited PEP moiety of the substituted dendrimers (see Table

TABLE 2: Values for the Fluorescence Anisotropy Measurements of the Nanostar and the Series of Compact-Perylene Dendrimers in Dichloromethane

molecule	r_0	A_∞	θ_0 (rad)	τ_r (ns)	D_r ($\times 10^7$ s^{-1})	τ_w (ns)	D_w ($\times 10^8$ s^{-1})
nanostar	0.32	0.30	0.53	8.5	2.0	0.70	1.2
W31-per	0.34	0.16	0.65	5.4	3.1	0.98	1.3
W63-per	0.33	0.33	0.51	6.8	2.5	0.84	0.9
W127-per	0.31	0.45	0.42	11.0	1.5	0.40	1.3

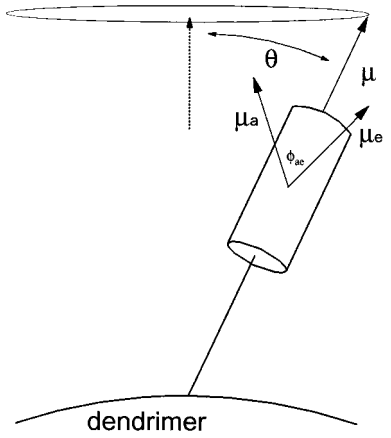

Figure 7. Schematic drawing of a cylindrical fluorescent probe "wobbling in a cone" about the central axis of the dendrimer macromolecule. The variable orientation angle θ is found experimentally to have a maximum value of θ_0. The absorption (μ_a) and emission (μ_e) dipoles are aligned about the central μ axis of the probe, with a common angle ϕ_{ae} between them.

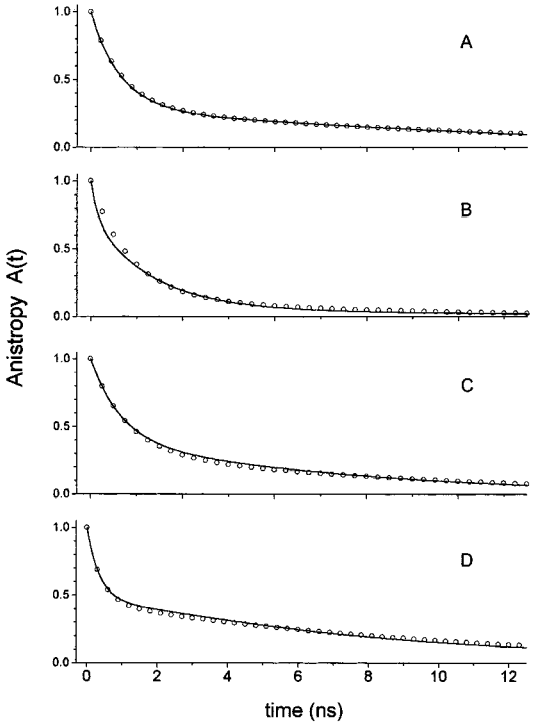

Figure 8. Calculation of $A(t)$ for the dendrimers in dichloromethane from experimental data (solid lines) and the best fits obtained from eq 6 (open circles). Curves are (A) nanostar, (B) W31-per, (C) W63-per, and (D) W127-per, with the fit parameters given in Table 2. Experimental $A(t)$ values were obtained from deconvolved best fits to the measured fluorescence polarization data (eq 8).

2), suggesting a similar dipolar alignment along the long molecular axis in these larger molecules.

Kinoshita et al.[16] have developed a theoretical treatment of fluorescence anisotropy of a macroscopically isotropic suspension of cylindrically symmetric fluorphores held within lipid bilayers. It is assumed that the symmetry axis of the fluorophore may rotate freely in a cone (wobble) at an angle θ with respect to the bilayer in which it is embedded, described by the rotational coefficient D_w. In addition, macromolecular rotation is observed, generally on a much longer time scale, with a rotational coefficient D_r. This model was generalized by Lipari and Szabo[17] to consider the two types of molecular motion as independent sources of the observed fluorescence depolarization. They found the long-time residual anisotropy of such a system to be

$$r_\infty = r_0 P_2(\cos \phi_a)\, P_2(\cos \phi_e) \langle P_2(\cos \theta) \rangle^2 \qquad (7)$$

where ϕ_a and ϕ_e are the angles between the absorption (μ_a) and emission (μ_e) transition dipoles with respect to the symmetry axis of the fluorophore (μ), respectively (see Figure 7.) $\langle P_2 \rangle$ is the expectation value of the second-order Legendre polynomial, and θ is the variable angle of wobble between the probe symmetry axis and its macromolecular host. In fairly rigid media, such as the fluorescent probe constrained within a lipid bilayer, the anisotropy may indeed decay to a long time value greater than zero, due to the inability of the probe to completely reorient. The dendrimers, although quite large and slowly moving, are ultimately capable of fully random rotational motion. However, for dendrimers of sufficiently large size (i.e., where $D_r < D_w$), the fluorescence depolarization of the perylenic trap may be adequately represented by this model. Additionally, it is important to have no competing depolarization mechanisms, such as Forster energy transfer, which can be maintained by use of sufficiently low probe concentration. The theoretical form of the time-dependent fluorescence anisotropy can be well approximated by[17]

$$A(t) = r(t)/r_0 = A_\infty \exp(-t/\tau_r) + (1 - A_\infty) \exp\{-t(1/\tau_r + 1/\tau_w)\} \qquad (8)$$

where τ_r and τ_w are the macromolecular rotation and probe wobbling times, respectively. The former can be estimated by eq 4, and a good approximation for the wobbling time[20] is

$$\tau_w = 7\theta_0^2/24D_w \qquad (9)$$

In conjunction with eq 7, the long time anisotropy factor $A_\infty = r_\infty/r_0$ can provide an upper bound for the semiangle of cone wobble, θ_0. For the particular case of our dendrimeric systems, if the dipolar angular values are taken to be $\phi_a = 0°$ and $\phi_e = 22°$, we have

$$A_\infty = 0.79[(3 \cos^2 \theta_o - 1)/2]^2 \qquad (10)$$

On the basis of this theoretical treatment, an examination of the dendrimer fluorescence depolarization data has been made, with the parameter results summarized in Table 2. Figure 8 gives the best fit fluorescence anisotropy $A(t)$ (open circles) to the deconvolved experimental data (solid lines). It should be noted that, on the time scale of these experiments, $A(t)$ does not decay

to a steady long time value (A_∞) for these systems. This is due in part to the limited time range of the experiments caused by the relatively short fluorescence lifetime of the probe, as well as to the unrestrained macromolecular rotation. The value of A_∞ was determined as a fitting parameter in eq 8 to the deconvolved experimental data. The fitted parameters can be discussed with respect to knowledge of the molecular structures. As their name implies, the compact dendrimers are smaller and more tightly packed than the corresponding extended molecule. Although the nanostar and W31-per are each composed of 4 dendrimer generations, the extended structure of the former leads to a larger molecular size, perhaps between that of the 5-generation W63-per and the 6-generation W127-per. Prior size-exclusion chromatography results[7] have suggested this to be the case, and the macromolecular rotation coefficient D_r obtained here verifies this further. If the dendrimers are assumed to be roughly spherical, then eq 4 suggests effective molecular radii of 2.4 nm for W31-per, 2.5 nm for W63-per, 2.7 nm for the nanostar, and 3.0 nm for W127-per. These values are very much as expected on the basis of molecular modeling and experimental data.

The wobbling time τ_w and semiangle θ_0 provide additional evidence of the solvated molecular structure. The smallest compact, W31-per, is expected to provide the least steric hindrance to the PEP trap rotation and is seen to have a fairly free motion with a semiangle of 37°. The somewhat more constrained motion in the nanostar may be due to the more floppy nature of the longer individual linear phenylacetylene chains, leading to folding over of the dendrimer backbone. The compacts show a monotonic decrease in cone angle with increasing generation number. The largest, W127-per, has a value that suggests significant structural overlap between the dendrimer backbone and the trap. Recent fluorescence lifetime data for these systems[21,25] agree well with this picture: the electronic excited-state fluorescence lifetime of the trap on the smaller dendrimers (e.g., W31-per and the nanostar) is very accurately fit by a single exponential of 2.2 ns in dichloromethane. For the larger species, these data become consecutively more nonexponential, and the best-fit lifetime is increased. In addition, measurements of exciton funneling rates to the trap following initial excitation into the dendrimer periphery do not show a monotonically inverse relationship with dendrimer size. Rather, the trapping rate for W127-per is more rapid than expected, suggesting a "short-circuit" pathway or exciton hopping directly from the outer generations to the perylenic trap.[21]

Additional fluorescence anisotropy data have been taken on the nanostar in dichloromethane, which can be used to obtain at least qualitative data on the intramolecular exciton hopping process. By exciting into the higher energy dendrimer states, the depolarization of the trap fluorescence indicates the angular relations between the dendrimer absorption dipole and the trap absorption and emission dipoles. Pumping at 378 nm selectively excites the innermost linear phenylacetylene chains attached to the molecular locus in dichloromethane. The time-dependent anisotropy is more difficult to analyze due to the competing depolarization processes of energy transfer and molecular motions. (Previous work has found that the hopping process cannot be viewed in the context of Forster transfer.[29] Rather, it appears to be a nearest-neighbor stochastic process, influenced strongly by the thermodynamic bias inherent in the nanostar's energy funnel.[9]) However, the trapping rates from this dendrimer state are significantly faster than the reorientational rates observed in this study,[21,30] permitting the determination of r_0. This value is proportional to $P_2(\cos\phi)$, where ϕ is the angular dipole overlap between the two electronic states.[17,31] The observed value of $r_0 = -0.09$ gives a loose approximation of 65° for ϕ in this case. This is particularly interesting considering the geometric structure of the nanostar: the lowest dendrimer states are meta-position-bonded (60° off collinearity) to the core phenyl group and thus to the central long axis of the trap.

Excitation into the nanostar periphery and into the compact dendrimer backbone was also conducted at 300 nm (all states of the compacts are composed of single unit diphenylacetylene chains, identical to the outermost generation of the extendeds). This permitted the observation of excitation depolarization due to exciton funneling through the entire dendrimer backbone. As might be expected, however, the resulting fluorescence was completely depolarized in all cases. Because of the multiple hopping steps between states of varying dipolar orientation, there was no observable polarization correlation.

The series of phenylacetylene dendrimers studied here provide an interesting application of the Kinoshita and Lipari−Szabo theory regarding measurement of macromolecular and intramolecular rotations via fluorescence depolarization. Although the approach was initially used to describe molecular reorientation constrained within a lipid bilayer, it can successfully be extended to the present case of free supermolecular motions in solvents. The time scale of the measurements, however, was limited by the radiative lifetime of the probe and could be extended significantly by an appropriate choice of substituent trap moiety. This choice is constrained by, among other requirements, the energy levels of the neighboring dendrimer states which produce the thermodynamic funneling characteristics of these molecules.

IV. Conclusion

Two lines of experimental approach have been used to study the characteristics of phenylacetylene dendrimers in solution. Both the steady-state and time-dependent excimer measurements, as well as those for the molecular reorientation dynamics, all give a unified picture of the solvated geometry for the dendrimers. These results can play a role in the prediction and calculation of the energetic funneling nature of these and similar supermolecules.

Acknowledgment. We acknowledge support for this research from the National Science Foundation, Division of Materials Sciences, Grant DMR-9410709 (RK) and from ARO MURI DAAG-55-97-1 (JSM).

References and Notes

(1) Junge, B. M.; McGrath, D. V. *Chem. Commun.* **1997**, *9*, 857.
(2) Tomalia, D. A.; Naylor, A. M.; Goddard, W. A. *Angew. Chem., Int. Ed. Engl.* **1990**, *29*, 138.
(3) Webber, P.-W.; Liu, Y.-J.; Devadoss, C.; Bharathi, P.; Moores, L. S. *Adv. Mater.* **1996**, *8*, 237.
(4) Kopelman, R.; Tan, W. *Appl. Spectrosc. Rev.* **1994**, *29*, 39.
(5) Fox, M. A. *Acc. Chem. Res.* **1992**, *25*, 569−74.
(6) Tan, W., Kopelman, R., Wang, X. F., Herman, B., Eds.; Wiley: New York, 1996; pp 407−475.
(7) Kopelman, R.; Shortreed, M.; Shi, Z.-Y.; Tan, W.; Xu, Z.; Moore, J. S.; Bar-Haim, A.; Klafter, J. *Phys. Rev. Lett.* **1997**, *78*, 1239−42.
(8) Swallen, S. F.; Shortreed, M. R.; Shi, Z.-Y.; Tan, W.; Xu, Z.; Devadoss, C.; Moore, J. S.; Kopelman, R. In *Dendrimeric Antenna Supermolecules with Multistep Directed Energy Transfer*; Prasad, P. N., Ed.; Plenum Press: New York, 1998.
(9) Shortreed, M. R.; Swallen, S. F.; Shi, Z.-Y.; Tan, W.; Xu, Z.; Devadoss, C.; Moore, J. S.; Kopelman, R. *J. Phys. Chem. B.* **1997**, *101*, 6318−22.
(10) Bar-Haim, A.; Klafter, J.; Kopelman, R. *J. Am. Chem. Soc.* **1997**, *26*, 66197.
(11) Tretiak, S.; Cherniak, V.; Mukamel, S. *J. Phys. Chem. B* **1998**, *102*, 3310−15.

(12) Swallen, S. F.; Shi, Z.-Y.; Tan, W.; Xu, Z.; Moore, J. S.; Kopelman, R. *J. Lumin.* **1998**, *76&77*, 193−6.
(13) Lindsey, J. S. *J. Am. Chem. Soc.* **1994**, *116*, 9759−60.
(14) Bignozzi, C. A.; Argazzi, R.; Schoonover, J. R.; Meyer, G. J.; Scandola, F. *Sol. Energy Sol. Cells* **1995**, *38*, 187−98.
(15) Balzani, V.; Campagna, S.; Denti, G.; Alberto, J.; Serroni, S.; Venturi, M. *Sol. Energy Sol. Cells* **1995**, *38*, 159−73.
(16) Kinoshita, K.; Kawato, S.; Ikegami, A. *Biophys. J.* **1977**, *20*, 289−305.
(17) Lipari, G.; Szabo, A. *Biophys. J.* **1980**, *30*, 489−506.
(18) Xu, Z.; Moore, J. S. *Acta Polym.* **1994**, *45*, 83.
(19) Press, W. H.; Flannery, B. P.; Teukolsky, S. A.; Vetterling, W. T. *Numerical Recipes in C*; Cambridge University Press: Cambridge, 1988.
(20) O'Connor, D. V.; Phillips, D. *Time Correlated Single Photon Counting*; Academic Press: Orlando, FL, 1984.
(21) Swallen, S. F.; Kopelman, R.; Moore, J. S. In *Energy Transfer in Organic Dendrimer Antenna Funnel and Anti-funnel Supermolecules*; Drake, J. M., Klafter, J., Grest, G. S., Kopelman, R., Eds.; *Proc. Mat. Res. Soc.* **1999**, *543*, 311−318.
(22) Shortreed, M. R.; Shi, Z.-Y.; Kopelman, R. *Mol. Cryst. Liq. Cryst.* **1996**, *283*, 95−100.
(23) Birks, J. B. *Photophysics of Aromatic Molecules*; Wiley-Interscience: New York, 1970.
(24) Birnbaum, D.; Kook, S. K.; Kopelman, R. *J. Phys. Chem.* **1993**, *97*, 3091−4.
(25) Swallen, S. F.; Kopelman, R.; Moore, J. S.; Devadoss, C. *J. Mol. Struct.* **1999**, *486*, 585−97.
(26) Parson, R. P.; Kopelman, R. *Chem. Phys. Lett.* **1982**, *87*, 528.
(27) Lakowicz, J. R.; Knutson, J. R. *Biochemistry* **1980**, *19*, 905.
(28) Christensen, R. L.; Drake, R. C.; Phillips, D. *J. Phys. Chem.* **1984**, *90*, 5960−7.
(29) Xu, Z.; Kahr, M.; Walker, K. L.; Wilkins, C. L.; Moore, J. S. *J. Am. Chem. Soc.* **1994**, *116*, 4537.
(30) Swallen, S. F.; Kopelman, R.; Xu, Z.; Moore, J. S. *Proc. Electrochem. Soc.* **1998**, *98*, 85−92.
(31) Kim, Y. R.; Share, P.; Pereira, M.; Sarisky, M.; Hochstrasser, R. M. *J. Chem. Phys.* **1989**, *91*, 7557−62.